Earth and Planetary Science Letters 619 (2023) 118309

Contents lists available at ScienceDirect

Earth and Planetary Science Letters

journal homepage: www.elsevier.com/locate/epsl

Crustal flow driving twin domes exhumation and low-angle normal faulting in the Menderes Massif of western Anatolia

Ömer Bodur [a,b,*], Oğuz Hakan Göğüş [a], Sascha Brune [c], Ebru Şengül Uluocak [d], Anne Glerum [c], Andreas Fichtner [e], Hasan Sözbilir [f]

[a] Eurasia Institute of Earth Sciences, Istanbul Technical University, Istanbul, Turkey
[b] Department of Geosciences, The University of Texas at Dallas, Richardson, Richardson, Dallas, 75080-3021, TX, United States of America
[c] Helmholtz-Centre Potsdam, GFZ German Research Centre for Geosciences, Telegrafenberg, D-14473, Potsdam, Germany
[d] Department of Geophysical Engineering, Çanakkale Onsekiz Mart University, Çanakkale, Turkey
[e] Department of Earth Sciences, ETH Zurich, Zurich, Switzerland
[f] Department of Geology, Engineering Faculty, Dokuz Eylül University, Bornova-Izmir, Turkey

ARTICLE INFO

Article history:
Received 23 February 2023
Received in revised form 23 June 2023
Accepted 8 July 2023
Available online 26 July 2023
Editor: R. Bendick

Keywords:
geodynamic modeling
lower crustal flow
western Anatolia

ABSTRACT

Lower crustal flow in regions of post-orogenic extension has been inferred to explain the exhumation of metamorphic core complexes and associated low-angle normal (detachment) fault systems. However, the origin of detachment faults, whether initially formed as high-angle or low-angle shear zones, and the extension is symmetric or asymmetric remains enigmatic. Here, we use numerical modeling constrained by geophysical and geological data to show that symmetric extension in the central Menderes Massif of western Anatolia is accommodated by the crustal flow. Our geodynamic model explains how opposite dipping Gediz and Büyük Menderes detachment faults are formed by ~40° footwall rotation. Model predictions agree with seismic tomography data that suggests updoming of lower crust beneath the exhumed massifs, represented as "twin domes" and a flat Moho. Our work helps to account for the genetic relation between the exhumation of metamorphic core complexes and low-angle normal faulting in both Cordillera and Aegean orogenic regions and has important implications on crustal dynamics in extensional provinces.

1. Introduction

Extensional tectonics following mountain building-orogenic-processes lead to special geological characteristics of the crust, such as rapid pulses of magmatism, exhumation of metamorphic core complexes, and associated low-angle normal (detachment) faults with tens of kilometers of displacements (Dewey, 1988; Malavieille, 1993; Jolivet, 2001; Rey et al., 2001; Lister et al., 1984). However, the extent and magnitude to which post-orogenic extension is involved in strain localization in the brittle upper crust and in ductile flow in the lower crust are not well understood. In this work, we test the hypothesis that the origin of central Menderes metamorphic core complex and symmetric detachment faulting in western Anatolia, a post-Alpine extended region, are formed by ductile flow of lower crust and footwall rotation of high-angle normal faults.

The exhumation of metamorphic rocks in the central Menderes Massif has been accommodated by two symmetrically developed, outward-facing ductile-brittle high strain (low-angle) detachment faults (<20°). The northern detachment fault, the Gediz/Alaşehir detachment, is associated with the top-to-the N-NNE shear sense, whereas the southern one is associated with the top-to-the S shear sense (Şengör, 1987; Hetzel et al., 1995; Emre and Sözbilir, 1997; Gessner et al., 2001; Bozkurt, 2001; Lips et al., 2001; Işık et al., 2003; Göğüş, 2004; Çemen et al., 2006; Nilius et al., 2019; Heineke et al., 2019b) (Fig. 1a, b). Proposed ages for the initiation of normal faulting for each detachment system vary spatially and temporally. For instance, based on isotopic dating along fault rocks/cataclasites, Hetzel et al. (2013), suggest that the onset of Büyük Menderes detachment faulting is ~22-20 Ma, whereas the shearing across the Gediz detachment began at ~16 Ma inferred from dating of syn-extensional intrusions (Catlos and Çemen, 2005; Glodny and Hetzel, 2007; Rossetti et al., 2017). Further, magnetostratigraphic analysis and isotopic ages over the supra-detachment basins suggest that these two detachments have operated simultaneously since 16 Ma (Şen and Seyitoğlu, 2009). A detachment-controlled symmet-

* Corresponding author.
E-mail address: omer.bodur@utdallas.edu (Ö. Bodur).

https://doi.org/10.1016/j.epsl.2023.118309
0012-821X/

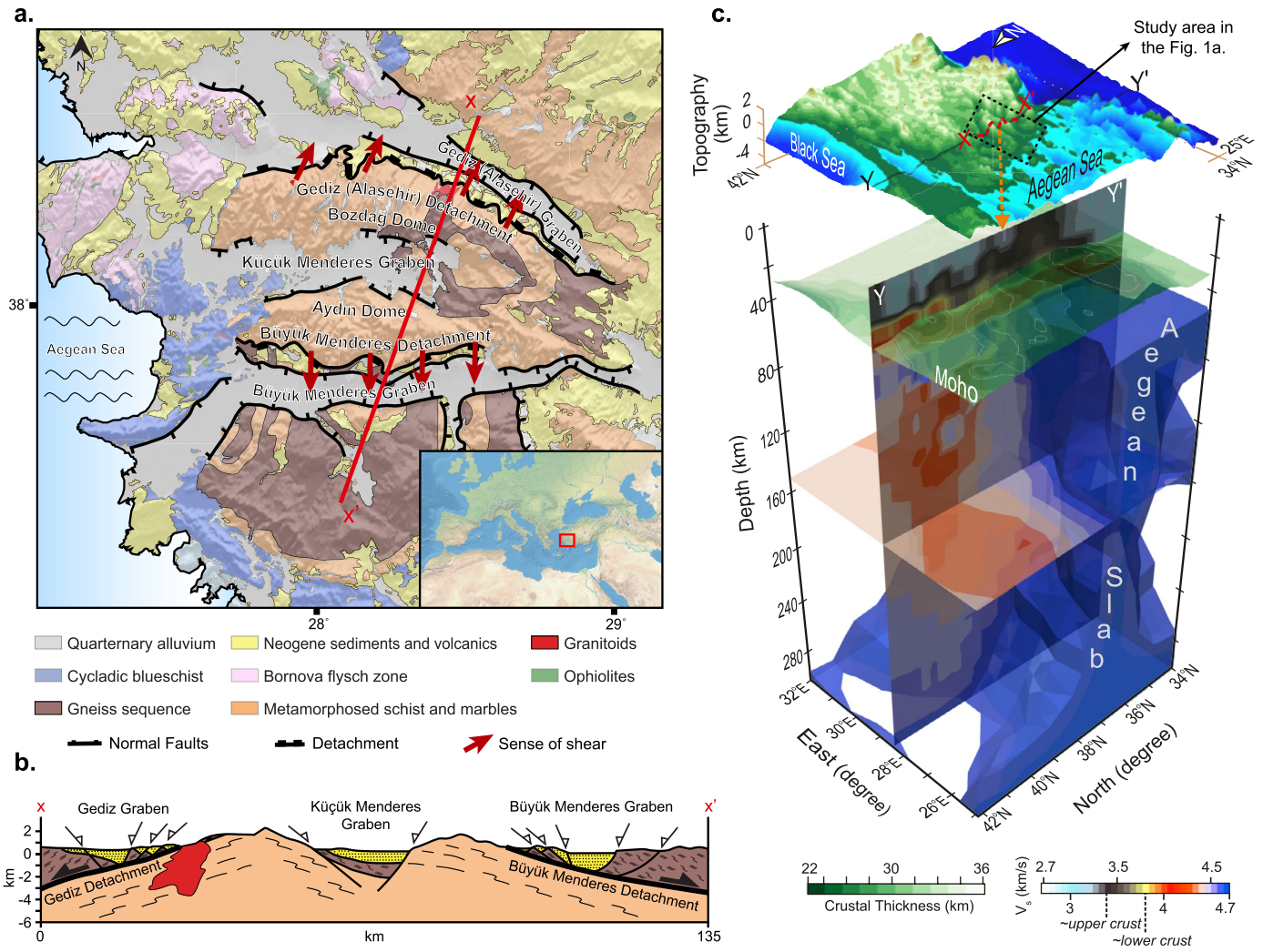

Fig. 1. a. Geological map of the central part of western Anatolia extensional region (Menderes Massif) that shows the main geological features discussed in this work. Metamorphosed schist and marble are footwall rocks and represented by greenschist to amphibolite facies metamorphics and the hangingwall rocks are described by high-grade metamorphics (Gneissic core). The map is based on the geological map of Türkiye (MTA, 2002), including the differentiation of metamorphic units, according to Lips et al. (2001) and Okay (2001) **b.** Simplified NNE-SSW cross section across the central Menderes Massif that shows bivergent detachment faults and symmetrically arranged exhumed massifs **c.** 3-D view of a seismic tomography model based on isotropic S velocities (Vs) across the crust as well as the upper mantle beneath western Anatolia (derived from Fichtner et al., 2013).

ric cooling pattern related to unroofing of central Menderes has also been suggested through thermochronological studies (Gessner et al., 2001; Ring et al., 2003). Such symmetric configuration of core complex exhumation has been interpreted with respect to the Küçük Menderes graben (rift), located above a central axis of a large-scale syncline where both detachments and the folding evolved contemporaneously (Gessner et al., 2001; Seyitoğlu et al., 2004).

While strain localization across exhumed ranges in the central Menderes Massif region is characterized by detachment faults, high-angle normal faults are well documented along the graben boundaries - akin to rifted margins (Fig. 1a,b). Based on field observations and seismic reflection data, a number of studies interpret that detachment faults in central Menderes were initially formed at higher dip angles ($> 30°$) and rotated to shallower orientations (Cohen et al., 1995; Bozkurt, 2000; Gessner et al., 2001; Seyitoğlu et al., 2002; Bozkurt and Sözbilir, 2004; Çiftçi and Bozkurt, 2010; Demircioğlu et al., 2010). Gessner et al. (2001) propose a rolling-hinge model to address the synchronous evolution of bivergent detachment fault systems. Namely, flexural isostatic footwall uplift is associated with fault rotation as well as the formation of younger high-angle normal faults on the hanging-wall of the main breakaway which successively rotates to low-angle shear zones (Buck, 1988; Wernicke and Axen, 1988). Accordingly, a rolling hinge type tectonic evolution for discrete shear zones in the footwall of the Gediz (Alaşehir) detachment (Seyitoğlu et al., 2002) and the Büyük Menderes detachment (Sümer et al., 2020; Türesin and Seyitoğlu, 2021) has been invoked through geologic mapping, stratigraphic analyses, and data from seismic reflection studies. On the other hand, Öner and Dilek (2011) suggests that the detachment fault was initially formed as a low-angle shear zone (without rotation) in which the early Miocene-late Pleistocene sediments of Alaşehir (Gediz) graben were deposited in a supradetachment basin. While the studies above provide a conceptual geological framework, however, the origin of core complex exhumation and evolution of ductile-to-brittle localized strain have not been addressed in the context of whole-crust extensional dynamics.

A multi-scale full seismic waveform inversion for crustal and upper-mantle structures by Fichtner et al. (2013) demonstrates that the upper crust of the Menderes Massif is associated with anomalously high velocities with respect to neighboring regions. This has led to the interpretation of upward displacement of the lower crust typically associated with higher velocities than the upper crust (Fig. 1c). Seismic analyses of Karabulut et al. (2013) also

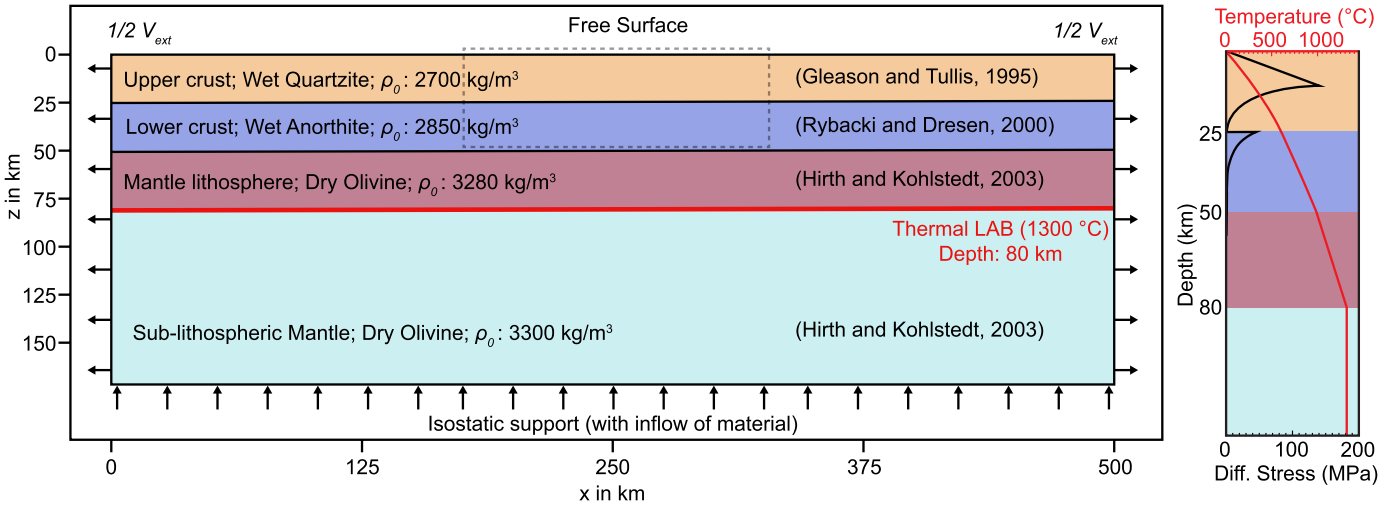

Fig. 2. Illustration of the model geometry, set-up, material properties, and density fields for the experiments. The corresponding strength profile for the initial conditions and a strain rate of 1×10^{-15} is shown on the right. The dashed rectangle outlines the area shown in Figs. 3 and 4. The density values given are the reference densities for each material.

imply a flow of lower crust beneath the central Menderes Massif, inferred from the locally flat Moho at ~25 km depth to accommodate isostatic compensation through lower crustal dynamics (Block and Royden, 1990). Further, a lower velocity upper crustal anomaly has been imaged beneath the Küçük Menderes graben (Fig. 1c) in addition to the updoming lower crustal material shown in the relatively long-wavelength (> 150 km) variations of the isotropic S velocities (Fichtner et al., 2013).

In this work, by using thermo-mechanical models we investigate the dynamics of the post-orogenic extension where lower crustal flow plays a key role in strain distribution. Specifically, the evolution of an array of high and low-angle normal faults is explored and a genetic relationship between these faults and the exhumation of lower crustal rocks is demonstrated. Further modeling is used to test the role of varying extension rates and reduced upper crustal strength. Results are reconciled with the last ~ 15 Ma evolution of the central Menderes Massif of western Anatolia, where symmetrically arranged detachment systems are prominent and seismological data suggests lower crustal flow. Overall, our work will provide new insight into how crustal dynamics control the tectonics of rifted margins and the evolution metamorphic core complexes around the globe.

2. Data and methods

2.1. Numerical technique, rheological characteristics, and model setup

To reach the objectives of this work, we use the finite element code ASPECT (Bangerth et al., 2020; Rose et al., 2017; Heister et al., 2017; Kronbichler et al., 2012), which has been extensively used for conducting geodynamical experiments ranging in scale from the crust to the deeper mantle. ASPECT is employed to solve the extended Boussinesq equations of momentum, mass, and energy as well as advection equations for each compositional field. We compute the 2-D visco-plastic deformation within the lithosphere and sub-lithospheric mantle of a model domain that is 500 km wide and 165 km deep (Fig. 2). Adaptive mesh refinement is used to adapt the precision and optimization of the computational calculations. We employ coarse, intermediate, and maximum resolutions beneath 50 km depth, between 50 and 20 km depth, and above 20 km depth, each represented by a resolution of 2500, 1250, and 625 m respectively.

In terms of rheological setup, the visco-plastic effective viscosity η_{eff} is computed from either a composite of dislocation and diffusion creep $\eta_{eff}^{diff|disl} = \frac{1}{2}(\frac{1}{A})^{1/n}\dot{\varepsilon}_e^{(1-n)/n}\exp(\frac{Q+PV}{nRT})$, or Drucker-Prager plasticity $\eta_{eff}^{pl} = \frac{C\cos(\phi)+P\ \sin(\phi)}{2\ \dot{\varepsilon}_e}$, depending on whether viscous stresses remain smaller than the yield stress or not (Glerum et al., 2018); with pressure P, temperature T, stress exponent $n = 1$ for diffusion creep and $n > 1$ for dislocation creep, pre-exponential factor A, the effective deviatoric strain rate $\dot{\varepsilon}_e = \sqrt{\frac{1}{2}\dot{\varepsilon}'_{ij}\dot{\varepsilon}'_{ij}}$, activation energy Q, activation volume V, gas-constant R, cohesion C, and friction angle ϕ (see Glerum et al., 2018 for numerical implementation and our supplement for employed parameter values).

The initial conditions of our model design aim to approximate the first-order lithospheric structure at the onset of normal faulting and exhumation in the central Menderes Massif region of western Anatolia, approximately 15 million years ago. The model accounts for four layers of materials: upper crust, lower crust, mantle lithosphere, and sub-lithospheric mantle (Table 1 and Fig. 2). The crustal domain consists of an upper crust (25 km thick) with wet quartzite rheology (Gleason and Tullis, 1995), and a lower crust (25 km thick) with wet anorthite rheology (Fig. 2) (Rybacki and Dresen, 2000). Our assumption of an initial 50 km thick crust is based on geological inferences (e.g., paleoelevation and metamorphic grades of exhumed rocks) (Şengör et al., 1985) in which extension in this region started after plate shortening by the Alpine orogeny. A relatively thin (30 km thick) mantle lithosphere is included in the model setup with dry olivine rheology (Hirth and Kohlstedt, 2003), since a number of geological studies suggest that portions of mantle lithosphere have been removed from beneath the western Anatolia (Aldanmaz et al., 2000; Ersoy et al., 2010; van Hinsbergen et al., 2010b; Gessner et al., 2013; Göğüş, 2015) through lithospheric delamination (Göğüş et al., 2017a; Göğüş and Ueda, 2018) or convective removal/lithospheric drip (Göğüş et al., 2017b).

2.2. Mechanical boundary conditions, thermal field and weakening effects

Kinematic boundary conditions are implemented by prescribing half of the extension velocity at each lateral model boundary. The top boundary is a free surface, while the bottom boundary features a free tangential motion in conjunction with a constant vertical inflow of material that balances the outflow through the lateral model sides. A constant temperature is prescribed at the top (0 °C) and bottom of the model domain (1300 °C), as well as

Table 1
Model parameters for reference experiment. *0.05 is used in experiment 4. Initial parameters of temperature=293 K, adiabatic surface temperature=1557 K, heat capacity=1200 Jkg−1K−1, internal friction angle=20°, cohesion=20 MPa, and grain size=1 mm are defined in all layers.

Parameter	Units	Upper Crust	Lower Crust	Lithospheric Mantle	Sub-Lithospheric Mantle
Reference Density	kgm^{-3}	2700	2850	3280	3300
Thermal expansivity	$10^{-5}K^{-1}$	2.7	2.7	3.0	3.0
Thermal diffusivity	$10^{-7}m^2s^{-1}$	7.7160	7.3099	8.3841	8.3333
Radiogenic heat production	μWm^3	1.5	0.2	-	-
Friction Weakening		0.1 and 0.05*	0.05	0.05	0.05
Cohesion strain weakening		0.05	0.05	0.05	0.05
Rheology		*Wet Quartzite*	*Wet Anorthite*	*Dry Olivine*	*Wet Olivine*
Pre-exponential constant for diffusion creep	$Pa^{-1}s^{-1}$	$5.97x10^{-19}$	$2.99x10^{-25}$	$2.25x10^{-9}$	$2.25x10^{-9}$
Grain size exponent		2.0	3.0	0	0
Activation energy for diffusion creep	$kj\ mol^{-1}$	223	159	375	375
Activation volume for diffusion creep	$cm^3\ mol^{-1}$	0	38.0	6.0	6.0
Pre-exponential constant for dislocation creep	$Pa^{-n}s^{-1}$	$8.57x10^{-28}$	$7.13x10^{-18}$	$6.52x10^{-16}$	$6.52x10^{-16}$
Power law exponent for dislocation creep		4.0	3.0	3.5	3.5
Activation energy for dislocation creep	$kj\ mol^{-1}$	223	345	530	530
Activation volume for dislocation creep	$cm^3\ mol^{-1}$	18.0	38.0	18.0	18.0

isolating boundaries at the sides. The initial temperature follows a steady-state geotherm in the lithosphere and an adiabat below. Radiogenic, shear heating, and adiabatic heating are included in the energy equation.

We include strain weakening/softening, where a strain-dependent friction angle and cohesion decrease linearly over a given strain interval (Huismans and Beaumont, 2003; Le Pourhiet et al., 2017), which is also predicted in progressive microscale numerical simulations (Dinç Göğüş et al., 2023). Here, the frictional weakening factor for the upper crust is set to 0.1 (for EXP-1, 2, 3) or 0.05 (EXP-4) over the accumulated plastic strain interval of 0 to 1. If strain exceeds 1, the friction angle and cohesion remain constant at their most weakened value.

We show two model suites where we investigate the impact of key parameters within a plausible range: (1) we vary the extension velocity between V_{ext} = 1-4 cm/year full rate and (2) we vary the friction angle strain weakening factor of the upper crust (0.1 - 0.05).

3. Results

We show predictions of four experiments selected from a series of numerical experiments (>100) in which the role of major controlling parameters on continental extension is examined. Details on the model design, including the initial temperature field and boundary conditions applied, are given in the methods section. Fig. 2 and Table 1 include further information on various parameters of the numerical experiments. The description of the section below begins with an explanation of the reference experiment (EXP-1) that best approximates the late Cenozoic geological evolution of the central Menderes Massif and follows with presentations of EXP-2, 3, and 4. Extension in the brittle crust begins through a random initial strain as a representation of deformation distribution which further evolves into strain localization. Results are only shown for the central part of the model domain, where the respective approximate distances of the central Menderes to the plate boundaries in the north and south are nearly close.

3.1. Evolution of core complex and the low-angle (detachment) faults

Fig. 3 shows the evolution of our reference experiment EXP-1, where V_{ext} = 2 cm/yr extension rate has been applied, which approximates present-day GPS-derived N-S extension in western Anatolia (Aktuğ et al., 2009). By 6 Myr (Fig. 3a), strain is localized along opposing conjugate shear bands/fault systems, dipping 50°-55° in the center of the model domain. Later by 12 Myr with more stretching (Fig. 3b), flow of the lower crust occurs where there is a higher magnitude of extension of the upper crust, beneath two major faults, owing to the lateral lithostatic pressure gradients. The net crustal thickness is now 30 km beneath the central region, expressed as approximately flat Moho, while there is lower crustal thickening and convergence beneath the zone of maximum upper crustal extension. The influx of crustal material accommo-

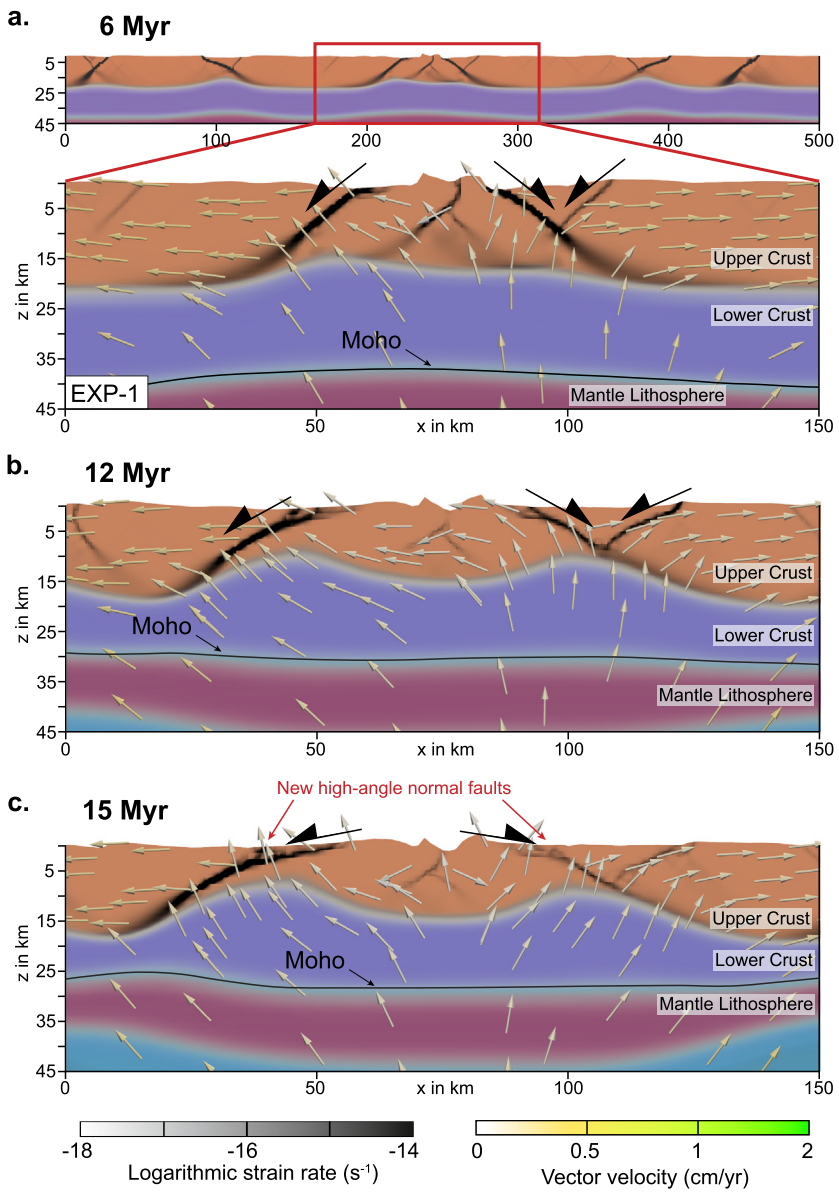

Fig. 3. Geodynamic evolution of our reference experiment (EXP-1) that approximates the last 15 Myr geological evolution of the central Menderes Massif of western Anatolia. Note that central part of the model domain is shown (150 km wide). Strain localization is interpreted in accordance with shear zone development where footwall rotation is associated with detachment fault evolution. The vectors show flow field over the experiment.

dates differential isostatic compensation, and upper portions of the shear zone rotate to shallower dips around two domal/antiformal cores. By 15 Myr (Fig. 3c), more rocks from the deeper crust are dragged upward near the surface along two major symmetrically (bivergent) arranged detachment systems, for instance, lower crustal rocks are exhumed as shallow as $<$10 km depth below the surface. The lowest dip angle of these faults near the surface is now $\sim$11°-14° and new high-angle normal faults develop on the hanging-wall of these main breakaway fault systems. Note that the Moho variation is uniformly sub-horizontal beneath the central domain although thinning of the upper crust is heterogeneous. For instance, there is a higher magnitude of stretching along upper (brittle) crustal extension above detachment faults, and below that there is a culmination of a twin-domes type core complex.

We test how variable rates of lithospheric extension can modify model predictions on the timescale of 15 Myr. These results may provide insight into the evolution of extensional tectonics both on the eastern and the western margin of the central Menderes, where the former margin accounts for lower and the latter for higher rates of extension due to its proximity to the central Aegean basin since subduction retreat has caused back-arc spreading (Jolivet and Brun, 2010; van Hinsbergen et al., 2010a).

EXP-2 shows the model development in which the extension rate is halved with respect to EXP-1 (so V_{ext} = 1 cm/yr) (Fig. 4a). The vertical flow and thickening of the lower crust and thinning of the upper crust are less pronounced, consequently, there is no significant core complex exhumation. By 15 Myr, the widespread distribution of shallow dipping normal faults across the entire crust does not develop, unlike in EXP-1, such fault plane rotation is very limited. The Moho variation remains subdued throughout the entire model domain and the strain localization mechanism may be characterized by wide rift type, in the sense defined by Buck (1991) and shown in numerical experiments of Brune et al. (2017).

On the other hand, with an increased extension velocity (V_{ext} = 4 cm/yr) in EXP-3, strain localization, ductile flow, and the associated exhumation of metamorphic cores and dome-like structures are accelerated (Fig. 4b). For instance, by 5 Myr there is up to $\sim$

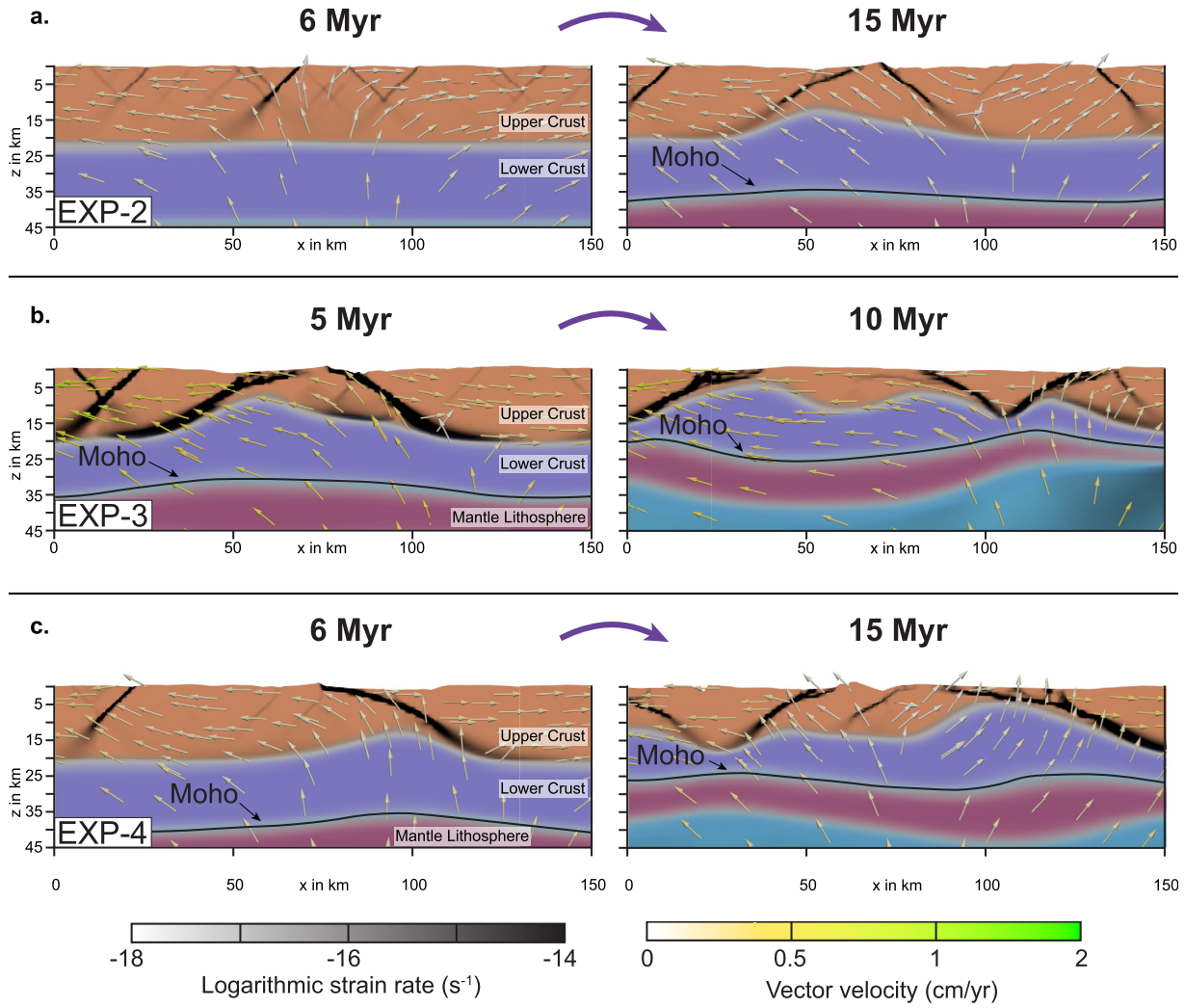

Fig. 4. Geodynamic evolution of EXP-2, 3, and 4. All model parameters are kept constant with respect to the reference experiment (EXP-1) except, **a.** in EXP-2 the extension rate (1 cm/yr), **b.** in EXP-3 the extension rate (4 cm/yr), and **c.** in EXP-4 the upper crustal strength is reduced by decreasing the frictional weakening to 0.05.

20 km lower crustal exhumation between closely spaced faults associated with shallow dip angles near the surface. By 10 Myr, the lower crust reaches the surface at the left limb of the symmetrically arranged detachment faults. Results show similarities with that of EXP-1, for example, oppositely dipping detachment systems warping around domal cores, however, the entire evolution develops much more rapidly. Note that the crustal thickness varies significantly across the model domain, for instance, it is undulated and thinned around the margins, nevertheless, the crustal thickness is almost constant beneath bivergent detachments where the upper crustal thinning is more amplified and the crustal flow process controls isostatic compensation.

In Fig. 4c we show the evolution of EXP-4 in which the strength of the upper crust is reduced by amplifying the frictional plastic strain softening. The motivation for such parameter change comes from previous studies where Huismans and Beaumont (2002) suggest that extensional tectonics may be symmetric or asymmetric depending on the implementation of this variable. By 6 Myr, instead of conjugate shear zone development, strain localizes along a specific shear zone, such as the one on the right side of the model where asymmetry prevails in earlier stages of the extension (Huismans and Beaumont, 2002). After 15 Myr, the unroofing of the metamorphic dome reaches ∼5 km depth below the surface as the deformation pattern becomes distinctly asymmetric by the development of a detachment zone across the brittle crust on the domed limb. This is similar to the simple shear extension model of Wernicke (1985), but a major detachment in our model soles in the lower crust rather than cutting through the lithosphere. Depending on the investigated width of the model domain, such extension type may also be symmetrical in terms of detachment fault development (Grasemann et al., 2012). Namely, another low-angle high strain shear zone develops (not shown in this frame), dipping in the opposite direction to the main shear zone, but it is in the distal end of the frame, 300 km further away from it. Although footwall rotation and the differential uplift of the lower crust are well pronounced in this experiment, we note that the results of EXP-4 do not account for the observed tectonics of the central Menderes region. For example, EXP-4 does not predict $<$100 km distance between Alaşehir/Gediz and Büyük Menderes detachment faults, symmetrical exhumation of metamorphic cores, and the flat Moho between these faults, inferred from seismological studies (e.g., Zhu et al., 2006; Fichtner et al., 2013; Karabulut et al., 2013).

4. Discussion

The results of the reference numerical experiment (EXP-1), where lower crustal flow is associated with footwall exhumation of “twin-domes” and rotation of steep normal faults in the upper crust into two major shallow-dipping high strain zones, comprise many of the first-order features that are invoked to explain the tec-

tonic evolution of the central Menderes metamorphic core complex in western Anatolia. Fig. 5a illustrates the spatial and structural agreement between the predicted bivergent tectonics in the form of an observed present-day axisymmetric array of low-angle shear zones projected across an N-S cross section of the region (see Fig. 1a X-X' for the location of the cross section). Further, the results satisfy the approximate distance between the Gediz (Alaşehir) (north) and Büyük Menderes (south) detachment faults and associated flanking and exhumation of "twin-domes shaped" footwall metamorphic rocks (Rey et al., 2011; Whitney et al., 2015). Moreover, the simulated geometry approximates the syncline/downward arc beneath Küçük Menderes graben in the center, with both detachments lying on the margin of this syncline. As the model predicts, there is no known detachment fault associated with the formation of Küçük Menderes (axial) graben where high-angle normal faults control its evolution since the Middle Miocene (Emre and Sözbilir, 2007; Rojay et al., 2005; Seyitoğlu and Işık, 2009; Bozkurt et al., 2008), similar to the formation of a localized and narrow rift in the distributed extensional domain (Brun and Choukroune, 1983).

Our model findings show that high-angle normal faults (50°-55°) have rotated progressively ∼40° to shallower dips about a horizontal axis accommodated by the crustal flow. This is consistent with several geological interpretations in western Anatolia. Namely, by interpreting the thermochronology data, cooling ages, and reconstruction of Eocene (flat) foliation planes to present day tilted structures, Gessner et al. (2001) suggest that the dip angle of both Gediz (Alaşehir) and Büyük Menderes detachment faults were initially 40°-60° during the earlier stages of post-Alpine extension. The higher dip angle origin of both Gediz (Alaşehir) and Büyük Menderes low-angle detachment faults has also been suggested through current (non-horizontal/tilted) dip angles of the bedding planes of syn-tectonic sedimentary strata, dipping towards the fault plane (Bozkurt, 2000; Sözbilir, 2001; Seyitoğlu et al., 2002; Sümer et al., 2020; Çiftçi and Bozkurt, 2010; Türesin and Seyitoğlu, 2021). According to fault plane restoration estimates, based on vertical distributed shear (Westaway and Kusznir (1993)) that develops contemporaneously with crustal extension and sedimentary deposition, the initial dip angle of the Büyük Menderes detachment ranges from 44° to 54° (Bozkurt, 2000), and an original dip of 56°-58° was estimated for the Gediz/Alaşehir detachment (Cohen et al., 1995). We note that during the model evolution a younger higher-angle normal fault forms on the hanging-wall of the low-angle detachment akin to rider blocks (Reston and Ranero, 2011; Choi and Buck, 2012). This new steeply dipping splay fault merges with the major detachment along the brittle-ductile transition while its dip angle reduces through time. In EXP-1 such a fault system starts to develop 12 Myr after model initiation, (e.g., comparable to 3-4 Ma before present in central Menderes geological evolution). The timing is in accord with the onset of higher-angle normal faults and the deposition of Late Miocene-Pliocene sediments proximal to the margin of the Gediz and Büyük Menderes grabens (Sarica, 2000; Bozkurt and Sözbilir, 2004; Kent et al., 2016).

Short wavelength ($\leq$150 km) variations of the crustal structures across the central Menderes Massif region are shown in Fig. 5b based on a regional high-resolution seismic tomography model (Fichtner et al., 2013). Notably, slow seismic velocities (Vs $<$ 3.4 km/s, $<$ 20 km depths, light blue region) in the upper part of the crust are observed in the center, beneath the Küçük Menderes graben to which lower crustal exhumation and detachment faulting have not been ascribed. However, on both margins of the Küçük Menderes graben, there are higher seismic velocities (3.4 $\leq$ Vs $\leq$ 3.8 km/s black and yellow regions) at shallower depths associated with the uprising of the lower crust (Fichtner et al., 2013; Çubuk-Sabuncu et al., 2017). This is consistent with findings of the EXP-1, where a twin-domes feature develops by crustal flow (Fig. 5a).

In Fig. 5a, we show the predicted Moho depth variation and it is sub-horizontal beneath the central Menderes Massif region where the Moho depth ranges from 25 to 28 km. Results of EXP-1 are mainly consistent with seismologically derived Moho variations for this part of western Anatolia's extended terrane (Zhu et al., 2006; Karabulut et al., 2013; Fichtner et al., 2013). It is worth noting that Moho beneath western Anatolia shows undulated pattern along the N-S transect, however, it is locally flat underneath the Menderes Massif. (Karabulut et al., 2013). Again, the flat Moho is controlled by the ductile flow of the mid-lower crust to isostatically compensate for the differential thinning of the upper crust and variations in crustal thickness, and this process has been suggested to account for the evolution of cordilleran core complexes in the western US and the Aegean region (Klemperer et al., 1986; Gans, 1987; Block and Royden, 1990; McKenzie et al., 2000; Tirel et al., 2004).

In Fig. 5c, we reconcile the exhumation history of the central Menderes Massif derived from low temperature thermochronological constraints against the predictions of EXP-1. For EXP-1, the exhumation rates are calculated (for every 1 Myr) through the trajectory of the lower crust at minimum depths with respect to the zero elevation (see yellow dots shown in the figure inset). These points on both domes correspond to the exhumed crust beneath the two detachment faults and follow approximately similar patterns and magnitudes since the beginning of the model (with uncertainties of $\pm$0.2 km/Myr). Namely, there is an increase in the exhumation rate between 15-10 Ma, from 1 km/Myr to ∼1.7 km/Myr and then it starts to decrease to ∼0.6 km/Myr by 5 Ma. The change after 5-0 is relatively minor and it is $>$ 1.0 km/Myr. Two-stage evolution predicted by the EXP-1 is in accord with the findings of Wölfler et al. (2017) for the exhumation of the footwall rocks of the Büyük Menderes detachment. According to the authors, the exhumation rate is ∼0.9 km/Myr during middle Miocene and it decreases to ∼0.43 km/Myr during the Miocene to Pliocene. For the footwall rocks of the Gediz detachment, Buscher et al. (2013) estimates that the rate of exhumation is 0.6-2 km/Myr and such variation is in the range of our model calculations.

We note that our models do not account for all geological processes involved in the late Cenozoic evolution of western Anatolia, such as surface erosion, partial melting of the lower crust, and plate rotation. For instance, based on thermochronological data and available erosion rates, Buscher et al. (2013) suggest that surface erosion also controls the exhumation and the landscape evolution of the Bozdağ dome, an exhumed range displaced by the Gediz detachment fault. Recent cosmogenic nuclides study by Heineke et al. (2019a) suggests that the erosion plays relatively minor role for rock exhumation along Gediz and Büyük Menderes (∼10% for the Gediz), however, it is more effective along both sides of the Küçük Menderes graben (∼50% rock exhumation). In our models, the flow of the lower crust, hence, the double dome formation (footwall exhumation) is mainly controlled by isostasy rather than lower crustal buoyancy. Rey et al. (2011) presents numerical experiments where partially molten lower crust becomes buoyant and double dome formation occurs with a small magnitude of extensional strain rate. Buoyancy driven dome formation may apply some of the cordilleran type metamorphic core complexes in North America where regional extension is decoupled from lower crustal flow under pure shear extension (Levy et al., 2023; Zuza and Cao, 2022). Although it may exert control to some degree, the purely buoyancy driven crustal upwelling model does not apply to the Aegean-west Anatolia, because the lithospheric extension in the region has been active since at least 15 Ma (Seyitoğlu and Scott, 1996; Bozkurt and Sözbilir, 2004; Çemen et al., 2006; Gessner et al., 2013; Roche et al., 2018; Heineke et al., 2019a,b). In brief, the isostatic foot-

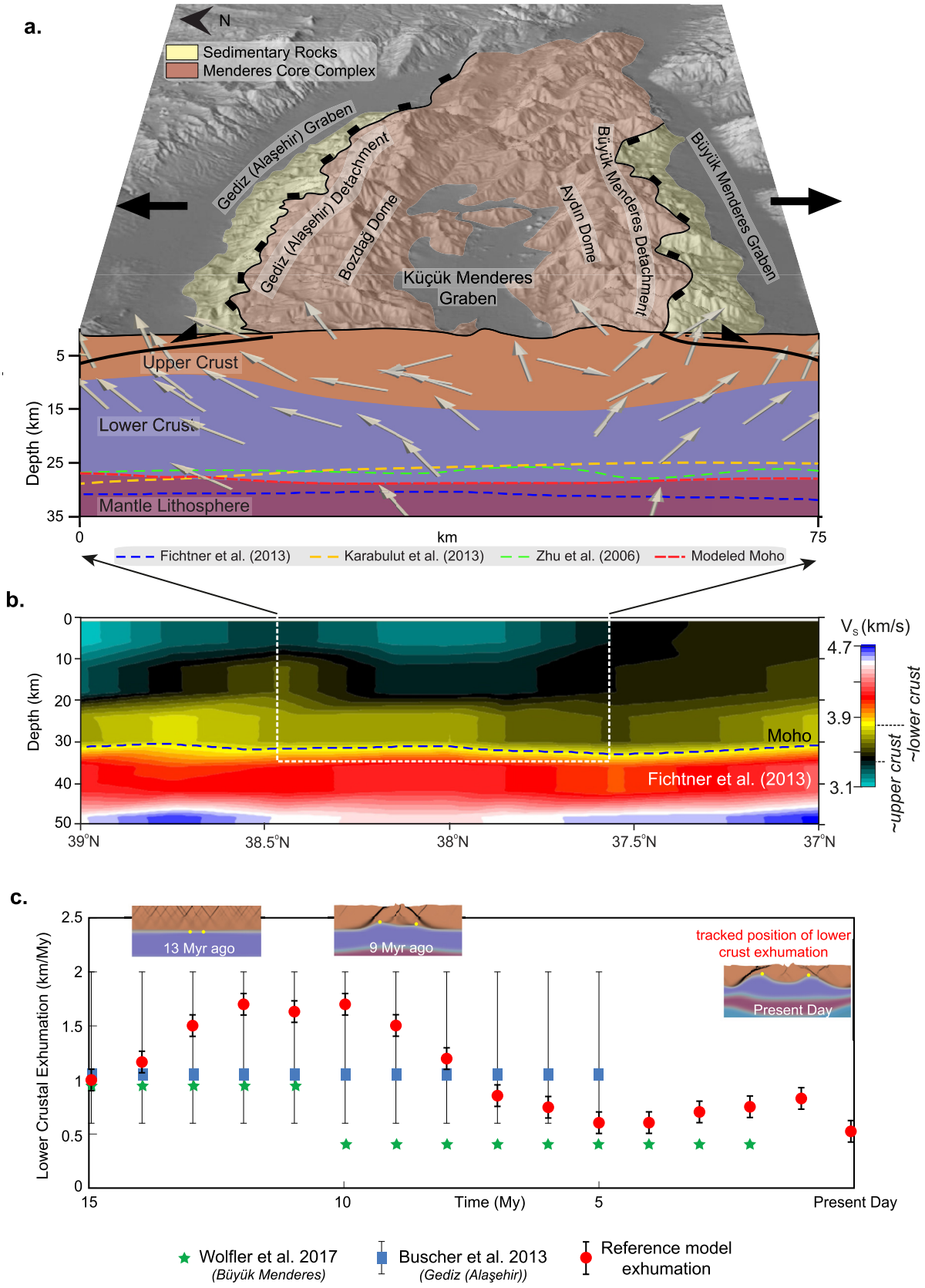

Fig. 5. Reconciling predictions of EXP-1 with geological, geophysical and thermochronological studies in the central Menderes massif of western Anatolia. **a.** NNE-SSW profile that shows the map projection of bivergent Gediz and Büyük detachment faults and their approximation to the model result. Note the agreement between modeled and observed Moho (see text for references). **b.** 2-D seismic (V_s) variations across the same profile of western Anatolia region to a depth of 50 km. Higher velocities in the shallow part of the crust (dark grey-black) are interpreted as the ascending of the normally associated lower crustal material. **c.** A diagram that shows the exhumation rate variation of the model and based on studies from low temperature thermochronology (Buscher et al., 2013 and Wölfler et al., 2017).

wall uplift by stretching is the primary mechanism driving twin dome formation in the area as predicted by our experiments in this work. Further, van Hinsbergen et al. (2010a) provides paleomagnetic evidence for a vertical axis rotation of ∼25°-30° in the central Menderes region with respect to the northern and southern part of the Menderes Massif to account for crustal exhumation and detachment faulting since ∼16 Ma. This would certainly be the focus of future 3-D modeling studies. Overall, the results of our reference experiment (EXP-1) are consistent with the present-day flat Moho inferred from seismological studies as well as with the twin-dome type exhumed massifs along bivergent detachment faults as documented by geological studies.

The exhumation of metamorphic core complexes and associated low-angle normal faults are common features of large-magnitude extensional provinces across Cordilleran and Mediterranean regions that develop in the terminal phase or in the aftermath of orogenesis. The results of this work in which progressive rotation of the high-angle normal faults to low-angle orientations as well as the exhumation of symmetrical (twin) domes are accommodated by the distributed flow of the lower crust may explain how post-orogenic lithospheric extension operates around the globe.

CRediT authorship contribution statement

Ömer Bodur: Conceptualization, Methodology, Software, Writing – original draft, Writing – review & editing, Investigation, Visualization. **Oğuz Hakan Göğüş:** Conceptualization, Investigation, Methodology, Supervision, Visualization, Writing – original draft, Writing – review & editing. **Sascha Brune:** Methodology, Resources, Software, Supervision, Visualization, Writing – original draft, Writing – review & editing. **Ebru Şengül Uluocak:** Writing – review & editing, Investigation, Methodology, Supervision, Software, Visualization, Writing – original draft. **Anne Glerum:** Methodology, Software, Supervision, Visualization, Writing – original draft, Writing – review & editing. **Andreas Fichtner:** Methodology, Supervision, Validation, Writing – original draft, Writing – review & editing. **Hasan Sözbilir:** Conceptualization, Supervision, Validation, Writing – original draft, Writing – review & editing.

Declaration of competing interest

The authors declare that they have no known competing financial interests or personal relationships that could have appeared to influence the work reported in this paper.

Data availability

Data will be made available on request.

Acknowledgements

We thank the Computational Infrastructure for Geodynamics (geodynamics.org) which is funded by the National Science Foundation under award EAR-0949446 and EAR-1550901 for supporting the development of ASPECT. The numerical experiments presented here are available through contacting the authors. Meanwhile, documentation and the details for the numerical code can be found online (at https://aspect.geodynamics.org). OHG, AF and EŞU acknowledge Anatolian Tectonics Project-ANATEC (funded by International Lithosphere Program). The authors gratefully acknowledge the computing time granted by the Resource Allocation Board and provided on the supercomputer Lise at NHR@ZIB as part of the NHR infrastructure. The calculations for this research were conducted with computing resources under the project bbp00039. We are grateful to Paul Kapp and an anonymous reviewer for their constructive comments on the manuscript. OHG acknowledges Turkish Academy of Sciences (TUBA) for GEBIP support and TUBITAK for 2219 fellowship programme. ACG is funded by a Helmholtz Recruitment Initiative.

Appendix A. Supplementary material

Supplementary material related to this article can be found online at https://doi.org/10.1016/j.epsl.2023.118309.

References

Aktuğ, B., Nocquet, J., Cingöz, A., Parsons, B., Erkan, Y., England, P., Lenk, O., Gürdal, M., Kilicoglu, A., Akdeniz, H., et al., 2009. Deformation of western Turkey from a combination of permanent and campaign GPS data: limits to block-like behavior. J. Geophys. Res., Solid Earth 114.

Aldanmaz, E., Pearce, J.A., Thirlwall, M., Mitchell, J., 2000. Petrogenetic evolution of late Cenozoic, post-collision volcanism in western Anatolia, Turkey. J. Volcanol. Geotherm. Res. 102, 67–95.

Bangerth, W., Dannberg, J., Gassmoeller, R., Heister, T., 2020. ASPECT v2.2.0, Zenodo. https://doi.org/10.5281/ZENODO.3924604.

Block, L., Royden, L.H., 1990. Core complex geometries and regional scale flow in the lower crust. Tectonics 9, 557–567.

Bozkurt, E., 2000. Timing of extension on the Büyük Menderes graben, western Turkey, and its tectonic implications. In: Special Publications, vol. 173. Geological Society, London, pp. 385–403.

Bozkurt, E., 2001. Late alpine evolution of the central Menderes massif, western Turkey. Int. J. Earth Sci. 89, 728–744.

Bozkurt, E., Sözbilir, H., 2004. Tectonic evolution of the Gediz graben: field evidence for an episodic, two-stage extension in western Turkey. Geol. Mag. 141, 63–79.

Bozkurt, E., Winchester, J.A., Ruffet, G., Rojay, B., 2008. Age and chemistry of miocene volcanic. Rocks from the Kiraz Basin of the Küçük Menderes graben: its significance for the extensional tectonics of southwestern Anatolia, Turkey. Geodin. Acta 21, 239–257.

Brun, J.P., Choukroune, P., 1983. Normal faulting, block tilting, and decollement in a stretched crust. Tectonics 2, 345–356.

Brune, S., Heine, C., Clift, P.D., Pérez-Gussinyé, M, 2017. Rifted margin architecture and crustal rheology: reviewing Iberia-newfoundland, central south Atlantic, and South China Sea. Mar. Pet. Geol. 79, 257–281.

Buck, W.R., 1988. Flexural rotation of normal faults. Tectonics 7, 959–973.

Buck, W.R., 1991. Modes of continental lithospheric extension. J. Geophys. Res., Solid Earth 96, 20161–20178.

Buscher, J., Hampel, A., Hetzel, R., Dunkl, I., Glotzbach, C., Struffert, A., Akal, C., Ratz, M., 2013. Quantifying rates of detachment faulting and erosion in the central Menderes massif (western Turkey) by thermochronology and cosmogenic 10be. J. Geol. Soc. 170, 669–683.

Catlos, E., Çemen, I., 2005. Monazite ages and the evolution of the Menderes massif, western Turkey. Int. J. Earth Sci. 94, 204–217.

Çemen, I., Catlos, E.J., Göğüş, O., Özerdem, C., 2006. Postcollisional extensional tectonics and exhumation of the Menderes massif in the western Anatolia extended terrane. Turkey.

Choi, E., Buck, W.R., 2012. Constraints on the strength of faults from the geometry of rider blocks in continental and oceanic core complexes. J. Geophys. Res., Solid Earth 117.

Çiftçi, N., Bozkurt, E., 2010. Structural evolution of the Gediz graben, SW Turkey: temporal and spatial variation of the graben basin. Basin Res. 22, 846–873.

Cohen, H., Dart, C., Akyüz, H., Barka, A., 1995. Syn-rift sedimentation and structural development of the Gediz and Büyük Menderes graben, western Turkey. J. Geol. Soc. 152, 629–638.

Çubuk-Sabuncu, Y., Taymaz, T., Fichtner, A., 2017. 3-d crustal velocity structure of western Turkey: constraints from full-waveform tomography. Phys. Earth Planet. Inter. 270, 90–112.

Demircioğlu, D., Ecevitoğlu, B., Seyitoğlu, G., 2010. Evidence of a rolling hinge mechanism in the seismic records of the hydrocarbon-bearing Alaşehir graben, western Turkey.

Dewey, J.F., 1988. Extensional collapse of orogens. Tectonics 7, 1123–1139.

Dinç Göğüş, Ö., Avşar, E., Develi, K., Çalık, A., 2023. Quantifying the rock damage intensity controlled by mineral compositions: insights from fractal analyses. Fractal Fract. 7 (5), 383.

Emre, T., Sözbilir, H., 1997. Field evidence for metamorphic core complex, detachment faulting and accommodation faults in the Gediz and Büyük Menderes grabens, western Anatolia. Iesca Proc. 1, 73–93.

Emre, T., Sözbilir, H., 2007. Tectonic evolution of the Kiraz Basin, Küçük Menderes graben: evidence for compression/uplift-related basin formation overprinted by extensional tectonics in west Anatolia. Turk. J. Earth Sci. 16, 441–470.

Ersoy, E.Y., Helvacı, C., Palmer, M.R., 2010. Mantle source characteristics and melting models for the early-middle Miocene mafic volcanism in western Anatolia: implications for enrichment processes of mantle lithosphere and origin of k-rich volcanism in post-collisional settings. J. Volcanol. Geotherm. Res. 198, 112–128.

Fichtner, A., Trampert, J., Cupillard, P., Saygin, E., Taymaz, T., Capdeville, Y., Villasenor, A., 2013. Multiscale full waveform inversion. Geophys. J. Int. 194, 534–556.
Gans, P.B., 1987. An open-system, two-layer crustal stretching model for the eastern great basin. Tectonics 6, 1–12.
Gessner, K., Gallardo, L.A., Markwitz, V., Ring, U., Thomson, S.N., 2013. What caused the denudation of the Menderes Massif: review of crustal evolution, lithosphere structure, and dynamic topography in southwest turkey. Gondwana Res. 24, 243–274.
Gessner, K., Ring, U., Johnson, C., Hetzel, R., Passchier, C.W., Güngör, T., 2001. An active bivergent rolling-hinge detachment system: central Menderes metamorphic core complex in western Turkey. Geology 29, 611–614.
Gleason, G.C., Tullis, J., 1995. A flow law for dislocation creep of quartz aggregates determined with the molten salt cell. Tectonophysics 247, 1–23.
Glerum, A., Thieulot, C., Fraters, M., Blom, C., Spakman, W., 2018. Non-linear viscoplasticity in aspect: benchmarking and applications to subduction. Solid Earth 9, 267–294.
Glodny, J., Hetzel, R., 2007. Precise u–pb ages of syn-extensional Miocene intrusions in the central Menderes Massif, western Turkey. Geol. Mag. 144, 235–246.
Grasemann, B., Schneider, D.A., Stöckli, D.F., Iglseder, C., 2012. Miocene bivergent crustal extension in the Aegean: evidence from the western Cyclades (Greece). Lithosphere 4, 23–39.
Göğüş, O.H., 2004. Geometry and Tectonic Significance of Büyük Menderes Detachment, in the Bascayir Area, Büyük Menderes Graben, Western Turkey. MSc. thesis. Oklahoma State University.
Göğüş, O.H., 2015. Rifting and subsidence following lithospheric removal in continental back arcs. Geology 43 (1), 3–6.
Göğüş, O.H., Ueda, K., 2018. Peeling back the lithosphere: controlling parameters, surface expressions and the future directions in delamination modeling. J. Geodyn. 117, 21–40.
Göğüş, O.H., Pysklywec, R.N., Faccenna, C., 2017a. Geodynamical models for continental delamination and ocean lithosphere peel away in an orogenic setting. In: Active Global Seismology: Neotectonics and Earthquake Potential of the Eastern Mediterranean Region, vol. 225, p. 121.
Göğüş, O.H., Pysklywec, R.N., Şengör, A.M.C., Gün, E., 2017b. Drip tectonics and the enigmatic uplift of the Central Anatolian Plateau. Nat. Commun. 8 (1), 1538.
Heineke, C., Hetzel, R., Nilius, N.P., Glotzbach, C., Akal, C., Christl, M., Hampel, A., 2019a. Spatial patterns of erosion and landscape evolution in a bivergent metamorphic core complex revealed by cosmogenic 10be: the central Menderes Massif (western Turkey). Geosphere 15, 1846–1868.
Heineke, C., Hetzel, R., Nilius, N.P., Zwingmann, H., Todd, A., Mulch, A., Wölfler, A., Glotzbach, C., Akal, C., Dunkl, I., et al., 2019b. Detachment faulting in a bivergent core complex constrained by fault gouge dating and low-temperature thermochronology. J. Struct. Geol. 127, 103865.
Heister, T., Dannberg, J., Gassmöller, R., Bangerth, W., 2017. High accuracy mantle convection simulation through modern numerical methods–ii: realistic models and problems. Geophys. J. Int. 210, 833–851.
Hetzel, R., Passchier, C.W., Ring, U., Dora, O., 1995. Bivergent extension in orogenic belts: the Menderes Massif (southwestern Turkey). Geology 23, 455–458.
Hetzel, R., Zwingmann, H., Mulch, A., Gessner, K., Akal, C., Hampel, A., Güngör, T., Petschick, R., Mikes, T., Wedin, F., 2013. Spatiotemporal evolution of brittle normal faulting and fluid infiltration in detachment fault systems: a case study from the Menderes Massif, western Turkey. Tectonics 32, 364–376.
Hirth, G., Kohlstedt, D., 2003. Rheology of the upper mantle and the mantle wedge: a view from the experimentalists. Geophys. Monogr., Am. Geophys. Union 138, 83–106.
Huismans, R.S., Beaumont, C., 2002. Asymmetric lithospheric extension: the role of frictional plastic strain softening inferred from numerical experiments. Geology 30, 211–214.
Huismans, R.S., Beaumont, C., 2003. Symmetric and asymmetric lithospheric extension: relative effects of frictional-plastic and viscous strain softening. J. Geophys. Res., Solid Earth 108.
Işık, V., Seyitoğlu, G., Çemen, I., 2003. Ductile–brittle transition along the Alaşehir detachment fault and its structural relationship with the Simav detachment fault, Menderes Massif, western Turkey. Tectonophysics 374, 1–18.
Jolivet, L., 2001. A comparison of geodetic and finite strain pattern in the Aegean, geodynamic implications. Earth Planet. Sci. Lett. 187, 95–104.
Jolivet, L., Brun, J.P., 2010. Cenozoic geodynamic evolution of the Aegean. Int. J. Earth Sci. 99, 109–138.
Karabulut, H., Paul, A., Afacan Ergün, T., Hatzfeld, D., Childs, D.M., Aktar, M., 2013. Long-wavelength undulations of the seismic Moho beneath the strongly stretched western Anatolia. Geophys. J. Int. 194, 450–464.
Kent, E., Boulton, S., Stewart, I., Whittaker, A., Alçiçek, M.C., 2016. Geomorphic and geological constraints on the active normal faulting of the Gediz (Alaşehir) graben, western turkey. J. Geol. Soc. 173, 666–678.
Klemperer, S.L., Hauge, T., Hauser, E., Oliver, J., Potter, C., 1986. The moho in the northern basin and range province, Nevada, along the cocorp 40 n seismic-reflection transect. Geol. Soc. Am. Bull. 97, 603–618.
Kronbichler, M., Heister, T., Bangerth, W., 2012. High accuracy mantle convection simulation through modern numerical methods. Geophys. J. Int. 191, 12–29.
Le Pourhiet, L., May, D.A., Huille, L., Watremez, L., Leroy, S., 2017. A genetic link between transform and hyper-extended margins. Earth Planet. Sci. Lett. 465, 184–192.
Levy, D.A., Zuza, A.V., Michels, Z.D., DesOrmeau, J.W., 2023. Buoyant doming generates metamorphic core complexes in the north American cordillera. Geology 51, 290–294.
Lips, A.L., Cassard, D., Sözbilir, H., Yilmaz, H., Wijbrans, J., 2001. Multi-stage exhumation of the Menderes massif, western Anatolia (Turkey). Int. J. Earth Sci. 89, 781–792.
Lister, G.S., Banga, G., Feenstra, A., 1984. Metamorphic core complexes of Cordilleran type in the Cyclades, Aegean Sea, Greece. Geology 12 (4), 221–225.
Malavieille, J., 1993. Late orogenic extension in mountain belts: insights from the basin and range and the late paleozoic variscan belt. Tectonics 12, 1115–1130.
McKenzie, D., Nimmo, F., Jackson, J.A., Gans, P., Miller, E., 2000. Characteristics and consequences of flow in the lower crust. J. Geophys. Res., Solid Earth 105, 11029–11046.
Nilius, N.P., Glotzbach, C., Wölfler, A., Hampel, A., Dunkl, I., Akal, C., Heineke, C., Hetzel, R., 2019. Exhumation history of the Aydın range and the role of the Büyük Menderes detachment system during bivergent extension of the central Menderes massif, western Turkey. J. Geol. Soc. 176, 704–726.
Okay, A.I., 2001. Stratigraphic and metamorphic inversions in the central Menderes massif: a new structural model. Int. J. Earth Sci. 89, 709–727.
Öner, Z., Dilek, Y., 2011. Supradetachment basin evolution during continental extension: the Aegean province of western Anatolia, Turkey. Bulletin 123, 2115–2141.
Reston, T., Ranero, C.R., 2011. The 3-d geometry of detachment faulting at mid-ocean ridges. Geochem. Geophys. Geosyst. 12.
Rey, P., Vanderhaeghe, O., Teyssier, C., 2001. Gravitational collapse of the continental crust: definition, regimes and modes. Tectonophysics 342, 435–449.
Rey, P.F., Teyssier, C., Kruckenberg, S.C., Whitney, D.L., 2011. Viscous collision in channel explains double domes in metamorphic core complexes. Geology 39, 387–390.
Ring, U., Johnson, C., Hetzel, R., Gessner, K., 2003. Tectonic denudation of a late cretaceous–tertiary collisional belt: regionally symmetric cooling patterns and their relation to extensional faults in the Anatolide belt of western Turkey. Geol. Mag. 140, 421–441.
Roche, V., Conand, C., Jolivet, L., Augier, R., 2018. Tectonic evolution of Leros (Dodecanese, Greece) and correlations between the Aegean domain and the Menderes massif. J. Geol. Soc. 175, 836–849.
Rojay, B., Toprak, V., Demirci, C., Süzen, L., 2005. Plio-quaternary evolution of the Küçük Menderes graben southwestern Anatolia, Turkey. Geodin. Acta 18, 317–331.
Rose, I., Buffett, B., Heister, T., 2017. Stability and accuracy of free surface time integration in viscous flows. Phys. Earth Planet. Inter. 262, 90–100.
Rossetti, F., Asti, R., Faccenna, C., Gerdes, A., Lucci, F., Theye, T., 2017. Magmatism and crustal extension: constraining activation of the ductile shearing along the Gediz detachment, Menderes massif (western Turkey). Lithos 282, 145–162.
Rybacki, E., Dresen, G., 2000. Dislocation and diffusion creep of synthetic anorthite aggregates. J. Geophys. Res., Solid Earth 105, 26017–26036.
Sarica, N., 2000. The plio-pleistocene age of Büyük Menderes and Gediz grabens and their tectonic significance on n-s extensional tectonics in west Anatolia: mammalian evidence from the continental deposits. Geol. J. 35, 1–24.
Şen, S., Seyitoğlu, G., 2009. Magnetostratigraphy of early–middle Miocene deposits from east–west trending Alaşehir and Büyük Menderes grabens in western Turkey, and its tectonic implications. In: Special Publications, vol. 311. Geological Society, London, pp. 321–342.
Şengör, A., Görür, N., Şaroğlu, F., 1985. Strike-slip faulting and related basin formation in zones of tectonic escape: Turkey as a case study.
Şengör, A.M.C., 1987. Cross-faults and differential stretching of hanging walls in regions of low-angle normal faulting: examples from western Turkey. In: Special Publications, vol. 28(1). Geological Society, London, pp. 575–589.
Seyitoğlu, G., Scott, B.C., 1996. The cause of ns extensional tectonics in western Turkey: tectonic escape vs back-arc spreading vs orogenic collapse. J. Geodyn. 22, 145–153.
Seyitoğlu, G., Tekeli, O., Çemen, I., Şen, Ş., Işık, V., 2002. The role of the flexural rotation/rolling hinge model in the tectonic evolution of the Alaşehir graben, western Turkey. Geol. Mag. 139, 15–26.
Seyitoğlu, G., Işık, V., Çemen, I., 2004. Complete tertiary exhumation history of the Menderes massif, western turkey: an alternative working hypothesis. Terra Nova 16, 358–364.
Seyitoğlu, V.G., Işık, V., 2009. Meaning of the Küçük Menderes graben in the tectonic framework of the central Menderes metamorphic core complex (western Turkey). Geol. Acta 7, 323–332.
Sözbilir, H., 2001. Extensional tectonics and the geometry of related macroscopic structures: field evidence from the Gediz detachment, western Turkey. Turk. J. Earth Sci. 10, 51–67.
Sümer, Ö., Sözbilir, H., Bora, U., 2020. Büyük Menderes grabeni'nin rolling hinge (yuvarlanan reze) modelinde supra-detachment (sıyrılma üstü) havzadan rift havzasına evrimi. Türk. Jeoloji Bül. 63, 241–276.
Tirel, C., Gueydan, F., Tiberi, C., Brun, J.P., 2004. Aegean crustal thickness inferred from gravity inversion. Geodynamical implications. Earth Planet. Sci. Lett. 228, 267–280.

Türesin, F.M., Seyitoğlu, G., 2021. Alaşehir type-rolling hinge mechanism in the northern margin of Büyük Menderes graben: evidence from seismic reflection and recent thermochronological data. Turk. J. Earth Sci. 30, 322–340.
van Hinsbergen, D.J., Dekkers, M.J., Bozkurt, E., Koopman, M., 2010a. Exhumation with a twist: paleomagnetic constraints on the evolution of the Menderes metamorphic core complex, western Turkey. Tectonics 29.
van Hinsbergen, D.J., Kaymakci, N., Spakman, W., Torsvik, T.H., 2010b. Reconciling the geological history of western Turkey with plate circuits and mantle tomography. Earth Planet. Sci. Lett. 297, 674–686.
Wernicke, B., 1985. Uniform-sense normal simple shear of the continental lithosphere. Can. J. Earth Sci. 22, 108–125.
Wernicke, B., Axen, G.J., 1988. On the role of isostasy in the evolution of normal fault systems. Geology 16, 848–851.
Westaway, R., Kusznir, N., 1993. Fault and bed 'rotation' during continental extension: block rotation or vertical shear? J. Struct. Geol. 15, 753–770.
Whitney, D.L., Roger, F., Teyssier, C., Rey, P.F., Respaut, J.P., 2015. Syn-collapse eclogite metamorphism and exhumation of deep crust in a migmatite dome: the p–t–t record of the youngest variscan eclogite (Montagne Noire, Trench massif central). Earth Planet. Sci. Lett. 430, 224–234.
Wölfler, A., Glotzbach, C., Heineke, C., Nilius, N.P., Hetzel, R., Hampel, A., Akal, C., Dunkl, I., Christl, M., 2017. Late Cenozoic cooling history of the central Menderes massif: timing of the Büyük Menderes detachment and the relative contribution of normal faulting and erosion to rock exhumation. Tectonophysics 717, 585–598.
Zhu, L., Mitchell, B.J., Akyol, N., Cemen, I., Kekovali, K., 2006. Crustal thickness variations in the Aegean region and implications for the extension of continental crust. J. Geophys. Res., Solid Earth 111.
Zuza, A., Cao, W., 2022. Metamorphic core complex dichotomy in the North American Cordillera explained by buoyant upwelling in variably thick crust. GSA Today.